Supplemental Information

For "Interferon-dependent IL-10 production by Tregs limits tumor Th17 inflammation" by Stewart *et al.*

Supplemental Methods

Mice

All knockout strains were obtained with or crossed onto C57BL/6 background. For *Ifnar1*$^{-/-}$, *Stat1*$^{-/-}$, *Stat2*$^{-/-}$, *Stat3* $^{fl/fl}$ mice, verification of background was performed by genome microsatellite mapping (Laboratory Animal Sciences Program, Frederick National Laboratory, Frederick, MD). *Ifnar1*$^{-/-}$ (1), *Stat1*$^{-/-}$ (2), *Stat2*$^{-/-}$ (3), *Myd88*$^{-/-}$ (4), *Wsx1*$^{-/-}$ (5) (Amgen Inc.), *Il10* $^{fl/fl}$ (6), *Il10r* $^{fl/fl}$ (7), *Tnf*$^{-/-}$ (8), FoxP3-EGFP (9), VERT-X (IL-10GFP) (10), *Stat3* $^{fl/fl}$ (11) and CD4-*Cre* mice (12) have been previously described. *Ifnar1*$^{-/-}$ mice were generously provided by Michel Aguet (Swiss Institute for Experimental Cancer Research, Lausanne, Switzerland), *Stat1*$^{-/-}$ and *Stat3* $^{fl/fl}$ mice were kindly donated by David Levy (New York University, New York, NY), *Stat2*$^{-/-}$ mice were a gift from Christian Schindler (Columbia University, New York, NY), *Myd88*$^{-/-}$ mice were provided by Shizuo Akira (Osaka University, Osaka, Japan), *Wsx1*$^{-/-}$ were a kind gift from Christian Saris (Amgen, Inc., Thousand Oaks, CA), *Tnf*$^{-/-}$ were provided by Sergei Nedospasov (Moscow State University, Moscow, Russia), FoxP3-EGFP were kindly given by Vijay Kuchroo (Harvard Medical School, Harvard, MA) and *Il23a*$^{-/-}$ (MGI Ref. J: 103485) were from Lexicon Genetics Mutant Mouse Regional Resource Center (The Woodlands, TX).

Antibodies for flow cytometry

Antibodies against CD11c (N418), CD8a (53-6.7), IL-17A-PerCP-Cy5.5 (rat IgG2a, eBio17B7), F480 (BM8), CD45 (30-F11), FoxP3-FITC (rtIgG2a, FJK-16s), IA-IE (M5/114.15.2), CD45.2 (104) were from eBioscience (San Diego, California), CD4 (GK1.5), CD3e (145-2C11), IL-10-APC (rat IgG2b, JES5-16E3), IAb (25-9-17), NK1.1 (PK136), CD11b (M1/70), CD19 (1D3), CD120b (TNFRII, TR75-89), TNF-PE (rat IgG1, MP6-XT22), IFN-γ-PE (rtIgG1, XMG1.2), CD45.1 (A20) were from BD Biosciences (Franklin Lakes, New Jersey), CD25 (PC61) and Ly6C (HK1.4) were from Biolegend (San Diego, California).

Real-time PCR

Taqman probe/primer sets obtained from Applied Biosystems (Life Technologies, Carlsbad, California) for quantification of gene expression were *Hprt* (Mm01545399_m1), *Il10* (Mm00439614_m1), *Il17a* (Mm00439619_m1), *Rorc* (Mm01261022_m1), *Nos2* (Mm00440502_m1), *Gzmb* (Mm00442834_m1), *Prf1* (Mm00812512_m1), *Il22* (Mm00444241), *Il1b* (Mm00434228_m1), *Cxcl1* (Mm04207460_m1), *Ptprc* (Mm01293575_m1), *Foxp3* (Mm00475162), *Il6* (Mm00446190), *Ccl20* (Mm01268754_m1), *Ccl22* (Mm00436439_m1), *Cx3cl1* (Mm00436454_m1) and *Ccl28* (Mm00445039_m1).

Supplemental References

1. Muller, U., Steinhoff, U., Reis, L.F., Hemmi, S., Pavlovic, J., Zinkernagel, R.M., and Aguet, M. 1994. Functional role of type I and type II interferons in antiviral defense. *Science* 264:1918-1921.
2. Durbin, J.E., Hackenmiller, R., Simon, M.C., and Levy, D.E. 1996. Targeted disruption of the mouse Stat1 gene results in compromised innate immunity to viral disease. *Cell* 84:443-450.
3. Park, C., Li, S., Cha, E., and Schindler, C. 2000. Immune response in Stat2 knockout mice. *Immunity* 13:795-804.
4. Adachi, O., Kawai, T., Takeda, K., Matsumoto, M., Tsutsui, H., Sakagami, M., Nakanishi, K., and Akira, S. 1998. Targeted disruption of the MyD88 gene results in loss of IL-1- and IL-18-mediated function. *Immunity* 9:143-150.
5. Yoshida, H., Hamano, S., Senaldi, G., Covey, T., Faggioni, R., Mu, S., Xia, M., Wakeham, A.C., Nishina, H., Potter, J., et al. 2001. WSX-1 is required for the initiation of Th1 responses and resistance to L. major infection. *Immunity* 15:569-578.
6. Roers, A. 2004. T Cell-specific Inactivation of the Interleukin 10 Gene in Mice Results in Enhanced T Cell Responses but Normal Innate Responses to Lipopolysaccharide or Skin Irritation. *Journal of Experimental Medicine* 200:1289-1297.
7. Pils, M.C., Pisano, F., Fasnacht, N., Heinrich, J.M., Groebe, L., Schippers, A., Rozell, B., Jack, R.S., and Muller, W. 2010. Monocytes/macrophages and/or neutrophils are the target of IL-10 in the LPS endotoxemia model. *Eur J Immunol* 40:443-448.
8. Kuprash, D.V., Tumanov, A.V., Liepinsh, D.J., Koroleva, E.P., Drutskaya, M.S., Kruglov, A.A., Shakhov, A.N., Southon, E., Murphy, W.J., Tessarollo, L., et al. 2005. Novel tumor necrosis factor-knockout mice that lack Peyer's patches. *Eur J Immunol* 35:1592-1600.
9. Bettelli, E., Carrier, Y., Gao, W., Korn, T., Strom, T.B., Oukka, M., Weiner, H.L., and Kuchroo, V.K. 2006. Reciprocal developmental pathways for the generation of pathogenic effector TH17 and regulatory T cells. *Nature* 441:235-238.
10. Madan, R., Demircik, F., Surianarayanan, S., Allen, J.L., Divanovic, S., Trompette, A., Yogev, N., Gu, Y., Khodoun, M., Hildeman, D., et al. 2009. Nonredundant roles for B cell-derived IL-10 in immune counter-regulation. *J Immunol* 183:2312-2320.
11. Raz, R., Lee, C.K., Cannizzaro, L.A., d'Eustachio, P., and Levy, D.E. 1999. Essential role of STAT3 for embryonic stem cell pluripotency. *Proc Natl Acad Sci U S A* 96:2846-2851.
12. Lee, P.P., Fitzpatrick, D.R., Beard, C., Jessup, H.K., Lehar, S., Makar, K.W., Perez-Melgosa, M., Sweetser, M.T., Schlissel, M.S., Nguyen, S., et al. 2001. A critical role for Dnmt1 and DNA methylation in T cell development, function, and survival. *Immunity* 15:763-774.
13. Sharov, A.A., Dudekula, D.B., and Ko, M.S. 2005. A web-based tool for principal component and significance analysis of microarray data. *Bioinformatics* 21:2548-2549.

Supplemental Figure Legends

Supplemental Figure 1: Expression of IL-10GFP by CD4$^+$CD25$^-$ and CD4$^+$CD25$^+$ Treg in organs of tumor-free VERT-X mice. Single cell suspensions from VERT-X reporter mice (black line) or WT (grey fill) were analyzed by flow cytometry. Electronic gating of singlet, vital dye$^-$ CD45$^+$ CD3$^+$ T cells was performed as indicated. In+Ax LN-Inguinal and Axillary lymph nodes; SI-small intestine; LI-large intestine; IEL-intraepithelial lymphocytes; LPL-lamina propria lymphocytes. Statistics show gated cell frequencies for one representative experiment of three.

Supplemental Figure 2: *Il10* and *Il17* expression in B16-F10 melanoma from total and T cell-conditional *Il10* knockout mice. Real-time quantitative PCR for *Il10* and *Il17a* on whole B16-F10 tumor tissue from indicated strains of mice. Box-and-whiskers plots are shown with (n) and p-values for two-tail unpaired Student's t-test with Welch's correction. ND – not detected.

Supplemental Figure 3: Tumor growth in T cell-conditional *Il10* knockout mice. Day 14 MC38 tumor volume is shown for indicated strains. Data are combined from three independent experiments. Graph shows mean ± SEM, (n) and p-values from two-tail unpaired Student's t-test with Welch's correction.

Supplemental Figure 4: Frequencies of CD4$^+$ T cells, Th1, Th17 and Treg in spleens from WT and *Il10*$^{-/-}$ mice. Single cell suspensions from spleens of indicated strains of MC38 tumor-bearing or tumor-free mice were stimulated with PMA and ionomycin and frequencies of IFN-γ^+FoxP3$^-$CD4$^+$ Th1 cells, IL17A$^+$FoxP3$^-$CD4$^+$ Th17 cells and IL10$^+$FoxP3$^+$ Treg were enumerated. Data in each column are from one experiment each. Frequencies are given as percentage of CD45$^+$ leukocytes. Statistics show mean and p-values for two-tail unpaired Student's t-test with Welch's correction.

Supplemental Figure 5: Relationship between *Il10* and *Il17a* expression in human head and neck squamous cell carcinoma. Public microarray datasets on cancer biopsies were selected based upon use of the Affymetrix chip platform and number of samples. Raw data were analysed using BRB Array tools and the JustRMA normalization method. Datasets showing inverse correlation between the *Il10* and *Il17a* probe sets are shown.

Supplemental Figure 6: Scheme for flow sorting of MC38 tumor Treg and identification of IL-10$^+$ cells. (A) Gating scheme for sorting of FSC/SSC/CD45$^+$/CD11b^{low}/CD3$^+$CD4$^+$CD25$^+$CD120b$^{+/low}$ cells. (B) Intracellular staining of FoxP3 (black line) or isotype control (grey fill) on Treg sorted as in (A) from indicated strains of mice. The combination of CD25 and the CD120b(TNFRII) markers identify populations from all strains that comprise approximately 95% FoxP3$^+$ Tregs. (C) Mesenteric lymph node cells from VERT-X mice were stimulated with PMA and ionomycin and IL-10GFP signal was compared with intracellular cytokine staining for IL-10 or isotype control on CD4+ T cells.

Supplemental Figure 7: Identification of genes differentially expressed by IL-10GFP$^+$ and IL-10GFP$^-$ MC38 tumor Treg by microarray analysis. Comparison of gene expression between IL-10GFP$^+$ and IL-10GFP$^-$ Treg from MC38 tumors. Agilent microarray analysis was performed on RNA from sorted VERT-X tumor Treg (IL-10GFP$^+$ and IL-10GFP$^-$ Treg from MC38 tumor. NIAArray tool (13) was used to identify genes differentially expressed between IL-10GFP$^+$ and IL-10GFP$^-$ Treg from MC38 tumor. Significant over- or under-expressed genes show significance by ANOVA at p<0.05 between triplicate samples. Data point for *Il10* is indicated.

Supplemental Figure 8: *Il10* correlated gene expression in Treg. Treg from VERT-X and FoxP3-EGFP spleen and MC38 tumor were sorted by flow cytometry and gene expression analysed by Agilent Microarray and NIA Array Tools. Gene expression across the panel of samples was correlated to *Il10* (Correlation threshold 0.7, fold-difference 1.5). Genes were filtered for statistical difference between VERT-X IL-10GFP$^+$ and IL-10GFP$^-$ groups (ANOVA using average error variance, p<0.05) and ranked according to correlation with *Il10*.

Supplemental Figure 9: CD4$^+$ T cell frequencies, Treg frequencies and IL-10$^+$ Treg in leukocytes from MC38 tumor implanted in gene knockout mice. Single cell suspensions from tumors of indicated knockout mice were stained for CD4 and FoxP3, or stimulated with PMA and ionomycin before intracellular staining with IL-10 and FoxP3. Frequencies of IL10$^+$FoxP3$^+$CD4$^+$ T cells, FoxP3$^+$CD4$^+$ T cells and CD4$^+$ T cells are given as percentage of CD4$^+$ T cells or as percentage of leukocytes. All data show one experiment performed except column four (data combined from three independent experiments). Statistical analysis for first column was performed by ANOVA with p-values > 0.05 for all pairwise comparisons and two-tail Student's t-test with Welch's correction for columns two-four.

Supplemental Figure 10: Microvessel density of MC38 tumors from T cell-conditional *Il10* knockout mice. CD34 staining on histological sections of MC38 tumors from indicated strains of mice was analysed by Aperio and box-and-whiskers plots showing calculated microvessel density are shown. Statistics show means ± SEM, (n) and p-values from two-tail unpaired Student's t-test with Welch's correction.

Supplemental Figure 11: Schematic showing relationships defined in this study. Type I IFN signaling is required for maintenance of signaling molecule (such as STAT1) expression levels. Type I IFN signaling promotes the accumulation of activated inflammatory Treg in the tumor microenvironment that display an activated phenotype. IL-10 expression by these Treg suppresses tumor Th17 inflammation including Th17 cells and Th17 cytokine expression.

Supplemental Tables

Supplemental Table 1: Expression of *Il10* by tumor Treg is associated with an activation gene signature. Genes showing significant differences in expression between IL-10GFP^{+} and IL-10GFP^{-} Tumor Treg from MC38 tumor in VERT-X mice as presented graphically in Figure 4.

Gene	Agilent Probe ID	Fold Change ($IL10^{+}/IL10^{-}$)	P (Actual)	P (Average)	FDR (Average)
Il10	A_51_P430766	25.04	0.001	<0.001	<0.01
Lag3	A_51_P264825	7.98	0.024	<0.001	<0.01
Pem	A_51_P376445	7.32	0.086	<0.001	0.03
Afm	A_52_P425734	6.26	0.036	0.003	0.53
Y08360	A_52_P291924	6.22	0.073	0.003	0.46
Abca8a	A_51_P379385	5.94	0.071	0.004	0.57
2010005H15Rik	A_51_P105380	5.55	<0.001	<0.001	<0.01
X97991	A_51_P290826	5.48	0.014	<0.001	<0.01
BC030910	A_51_P153063	5.06	0.004	0.001	0.32
Stfa1	A_51_P384894	4.77	0.016	0.006	0.72
AK005337	A_51_P466288	3.11	0.097	<0.001	0.07
BQ937878	A_51_P387769	3.11	0.050	0.002	0.33
AK044270	A_51_P311648	2.76	0.070	<0.001	<0.01
Cxcr6	A_51_P412027	2.50	0.006	<0.001	0.01
Prf1	A_52_P335178	2.47	0.072	<0.001	0.04
2210022N24	A_52_P628741	2.22	0.029	<0.001	0.08
AK013685	A_51_P287691	2.01	0.037	0.003	0.45
Gzmb	A_51_P333274	2.01	0.039	<0.001	0.05
Slc37a2	A_51_P259774	1.94	0.054	0.007	0.86
Ccl5	A_51_P485312	1.93	0.087	0.001	0.30
Nkg7	A_51_P499195	1.91	0.018	0.001	0.32
D830039D11	A_52_P344290	1.88	0.091	0.004	0.57
Rin3	A_51_P111562	1.87	0.088	0.002	0.41
Ccr5	A_52_P578732	1.87	0.041	0.003	0.47
1010001B04	A_52_P638459	1.86	0.050	0.002	0.40
Nkg7	A_52_P24447	1.83	0.058	0.004	0.55

NP063865	A_52_P74680	1.82	0.020	0.003	0.47
NAP052693-1	A_52_P444162	1.82	0.043	0.004	0.59
Rnase4	A_51_P237383	1.78	0.017	0.007	0.84
NAP111894-1	A_52_P286166	0.57	0.057	0.004	0.60
Sit	A_51_P144632	0.57	0.052	0.006	0.76
M55181	A_51_P102987	0.55	0.018	0.003	0.51
Gata3	A_52_P546363	0.55	0.068	0.002	0.44
AK018691	A_51_P192501	0.55	0.098	0.003	0.49
Bdh	A_51_P163106	0.53	0.096	0.004	0.58
Ebi2	A_51_P358683	0.51	0.001	0.001	0.32
Cables1	A_51_P117581	0.51	0.007	0.005	0.65
2900002K07	A_52_P466853	0.51	0.031	0.001	0.19
Stat4	A_51_P177092	0.51	0.021	0.003	0.51
NP050138	A_52_P184629	0.49	0.079	0.007	0.84
Pacsin1	A_51_P220422	0.49	0.012	0.007	0.86
Emb	A_51_P382849	0.49	0.003	0.001	0.22
AF152371	A_52_P238230	0.48	0.023	0.002	0.33
Mox2	A_52_P254095	0.48	0.048	0.004	0.54
Cd83	A_51_P199135	0.47	0.001	<0.001	0.07
D4Bwg1540e	A_51_P369690	0.46	0.004	0.008	0.86
1500031H04Rik	A_51_P350748	0.46	0.071	0.001	0.23
Pcsk1	A_52_P500979	0.46	0.010	0.002	0.36
X01643	A_52_P1158254	0.46	0.068	0.002	0.35
H2-Oa	A_51_P449329	0.45	0.055	0.002	0.33
A830050A14	A_52_P448870	0.45	0.006	0.001	0.32
C630019N20	A_52_P352277	0.44	0.040	0.002	0.33
ENSMUST00000022242	A_52_P10622	0.43	0.009	<0.001	0.07
Map17	A_51_P491329	0.42	0.001	0.001	0.19
Actg2	A_51_P241269	0.42	0.037	0.001	0.17
A430105L20	A_52_P279425	0.42	0.053	0.002	0.37
B230317C12Rik	A_51_P264527	0.41	0.039	0.004	0.58

AJ249820	A_52_P1078023	0.41	0.097	0.002	0.38
ENSMUST00000025192	A_51_P449325	0.40	0.010	<0.001	0.09
ENSMUST00000031927	A_52_P1078018	0.40	0.075	<0.001	0.10
BC064078	A_52_P812362	0.40	0.004	0.001	0.32
C030046M14	A_52_P188042	0.39	0.007	<0.001	0.10
3200002B17	A_52_P410449	0.38	0.028	0.003	0.49
Ramp3	A_51_P227090	0.37	0.003	<0.001	<0.01
C030046M14Rik	A_51_P320930	0.37	0.021	0.004	0.54
Ccr4	A_51_P444473	0.36	0.074	<0.001	0.13
X02333	A_51_P171075	0.36	0.068	0.001	0.17
M35131	A_51_P300657	0.35	0.013	0.002	0.42
NAP040554-1	A_52_P484194	0.34	0.003	<0.001	<0.01
AK051895	A_51_P503993	0.31	0.086	0.001	0.24
Lta	A_51_P351015	0.30	0.068	<0.001	<0.01
AF421198	A_52_P627116	0.30	0.038	0.001	0.23
Pcsk1	A_52_P164524	0.30	0.073	0.001	0.30
1110019A15	A_52_P592909	0.29	0.003	<0.001	<0.01
Il18r1	A_51_P505617	0.29	0.002	<0.001	<0.01
Il18rap	A_52_P517098	0.28	0.002	<0.001	0.01
BC023117	A_51_P438083	0.27	0.006	0.001	0.16
Dgat2	A_52_P359739	0.27	0.002	<0.001	<0.01
2410008J05	A_52_P402394	0.27	0.043	0.003	0.47
Marco	A_51_P371750	0.26	0.020	0.007	0.86
Slc6a13	A_52_P221824	0.26	0.001	<0.001	0.10
Dgat2	A_51_P396003	0.26	0.004	<0.001	<0.01
AK017900	A_51_P377171	0.25	0.029	<0.001	<0.01
Tnfrsf25	A_52_P460584	0.25	0.001	<0.001	<0.01
AK004390	A_51_P500002	0.24	0.001	<0.001	0.13
Ccr7	A_51_P420229	0.24	<0.001	<0.001	<0.01
Brp17	A_51_P372141	0.24	0.029	<0.001	0.02
Btla	A_51_P402359	0.23	0.002	0.001	0.17

Dcl1	A_51_P182311	0.22	0.035	0.002	0.37
D16847	A_52_P177324	0.22	0.075	0.009	1.00
Soat2	A_51_P196997	0.21	0.072	0.008	0.89
Ltf	A_51_P188141	0.21	0.004	<0.001	<0.01
AK030707	A_51_P147024	0.20	<0.001	<0.001	<0.01
A230077J24	A_52_P488666	0.20	0.039	<0.001	0.03
Tnfrsf25	A_51_P178561	0.20	0.005	<0.001	<0.01
Snai3	A_51_P356186	0.19	0.011	0.007	0.86
Ltf	A_52_P15388	0.19	0.006	<0.001	<0.01
D030014K03	A_52_P607060	0.18	0.004	0.009	1.00
1110061N23Rik	A_51_P217123	0.18	0.072	0.002	0.39
NAP026456-1	A_52_P556448	0.18	<0.001	<0.001	<0.01
ENSMUST00000023717	A_52_P665240	0.18	<0.001	<0.001	<0.01
A_52_P362072	A_52_P362072	0.17	0.042	0.007	0.86
Tff1	A_51_P504884	0.16	0.001	<0.001	<0.01
Il17rb	A_51_P464838	0.15	0.025	0.002	0.44
Dscam	A_51_P189943	0.15	0.004	0.004	0.60
1810009J06Rik	A_51_P502075	0.15	0.020	0.004	0.54
Tnp2	A_51_P321449	0.15	0.001	<0.001	0.01
AB041591	A_51_P489720	0.14	0.042	0.002	0.33
Atp1a2	A_52_P227267	0.14	0.003	0.002	0.39
AK029364	A_51_P385892	0.14	0.003	<0.001	<0.01
Nrgn	A_51_P171832	0.12	0.054	<0.001	0.01
Ccl1	A_51_P299896	0.12	0.016	<0.001	<0.01
Lad1	A_51_P116932	0.09	0.003	<0.001	<0.01
Scin	A_51_P335460	0.07	0.001	<0.001	<0.01
Prm2	A_51_P138705	0.06	0.003	<0.001	<0.01
4732472I07	A_52_P585907	0.05	<0.001	<0.001	<0.01
Ccr6	A_51_P388281	0.03	0.022	<0.001	<0.01

Supplemental Table 2: Gene sequences used for gene specific probes in nCounter analysis (Nanostring Technologies)

Gene	Accession Number	Targeted Region	Target Sequence
Ccr6	NM_009835.3	585-685	CTGGGGAATGAATTCCACAGAGTCCTACTTTGGAACGGATGATTATGACA ACACAGAGTATTATTCTATTCCTCCAGACCATGGGCCATGCTCCCTAGAA
Ccr7	NM_007719.2	755-855	CCCAGATGGTTTTTGGGTTCCTAGTGCCTATGCTGGCTATGAGTTTCTGC TACCTCATTATCATCCGTACCTTGCTCCAGGCACGCAACTTTGAGCGGAA
Foxp3	NM_054039.1	150-250	CCAGCTCCCGGCAACTTCTCCTGACTCTGCCTTCAGACGAGACTTGGAA GACAGTCACATCTCAGCAGCTCCTCTGCCGTTATCCAGCCTGCCTCTGACA
Gapdh	NM_001001303.1	890-990	AGGTTGTCTCCTGCGACTTCAACAGCAACTCCCACTCTTCCACCTTCGATG CCGGGGCTGGCATTGCTCTCAATGACAACTTTGTCAAGCTCATTTCCTG
Gata3	NM_008091.3	1943-2043	CATGCGTGAGGAGTCTCCAAGTGTGCGAAGAGTTCCTCCGACCCCTTCTA CTTGCGTTTTTCGCAGGAGCAGTATCATGAAGCCCGAAAGCGACAGATCT
Hprt1	NM_013556.2	30-130	TGCTGAGGCGGCGAGGGAGAGCGTTGGGCTTACCTCACTGCTTTCCGGA GCGGTAGCACCTCCTCCGCCGGCTTCCTCCTCAGACCGCTTTTTGCCGCGA
Icos	NM_017480.1	142-242	TTCACAATGGAGGTGTACAGATTTCTTGTAAATACCCTGAGACTGTCCAGC AGTTAAAAATGCGATTGTTCAGAGAGAGAGAAGTCCTCTGCGAACTCAC
Il10	NM_010548.1	985-1085	GGGCCCTTTGCTATGGTGTCCTTTCAATTGCTCTCATCCCTGAGTTCAGA GCTCCTAAGAGAGTTGTGAAGAAACTCATGGGTCTTGGGAAGAGAAACCA
Il17a	NM_010552.3	205-305	ACCTCAAAGTCTTTAACTCCCTTGGCGCAAAAGTGAGCTCCAGAAGGCCC TCAGACTACCTCAACCGTTCCACGTCACCCTGGACTCTCCACCGCAATGA
Il1rl1	NM_001025602.2	815-915	ATAGGAAAACCAGCAAGTATTGCCTGTTCAGCTTGCTTTGGCAAAGGCTC TCACTTCTTGGCTGATGTCCTGTGGCAGATTAACAAAACAGTAGTTGGAA
Il22	NM_016971.1	477-577	AGAAGAATGTCAGAAGGCTGAAGGAGACAGTGAAAAAGCTTGGAGAGAG TGGAGAGATCAAGGCGATTGGGGAACTGGACCTGCTGTTTATGTCTCTGAG
Lta	NM_010735.1	1115-1215	AAGAGGGGAAAAATAGAAAGCCGTCAGATGACAACTAGGTCCCAGACAC AAAGGTGTCTCACCTCAGACAGGACCCATCTAAGAGAGAGATGGCGAGAGA
Maf	NM_001025577.2	43-143	CTGGCAATGAACAATTCCGACCTGCCCACCAGTCCCCTGGCCATGGAAT ATGTTAATGACTTCGATCTGATGAAGTTTGAAGTGAAAAAGGAACCGGTGG
Rorc	NM_011281.2	1687-1787	CTTTCCCTTTCTGCACTCTATGAAGGGTGGTATCCCTAGGAGTAAGCAAA TCCTAAGACTGATTTTCTGCCCCTAGGCTTGCCTTGTAGGACAACAGCAG
Rpl30	NM_009083.4	14-114	CCCCGGCCATCTTGGCGGCTGGTGTTGGTGAGTGAGCTCTGCGGGGTAA ACGATTAGGCGGCTCGGGGAGCTCCGCTAGCTGGTGTTTGACGCTCTGGAT
Rpl9	NM_011292.2	240-340	GGTAACAGAAAGGAACTGGCCACCGTCAGGACCATCTGCAGTCATGTTCA GAACATGATCAAGGGTGTCACGCTGGGCTTCCGATACAAGATGCGGTCTG
Smad3	NM_016769.3	1845-1945	GTGTATCGCCACCTGACTCCTTGTTTAATGACAGAGGTCTGGGATGTCAC AGTCCAAAAGGAAAGTGCCTTTCTCCATGGCTGGAGTATGGAGTTTACCT
Socs2	NM_007706.3	1372-1472	TGCCTTTGTTTTTTGGGTTCCTATGCACTGGGTCAAAAGTCCAAGCTCCAT AGGAGAGAAAGAAAGGCTTCCATTTCCAGGAGGACAGCTGAAGGAGGGA
Socs3	NM_007707.2	585-685	CCGCGACAGCTCGGACCAGCGCCACTTCTTCACGTTGAGCGTCAAGACCC AGTCGGGGACCAAGAACCTACGCATCCAGTGTGAGGGGGGCAGCTTTTCG
Stat1	NM_009283.3	1590-1690	ACGCTGGGAACAGAACTAATGAGGGGCCTCTCATTGTCACCGAAGAACTT CACTCTCTTAGCTTTGAAACCCAGTTGTGCCAGCCAGGCTTGGTGATTGA

Supplemental Figure 1

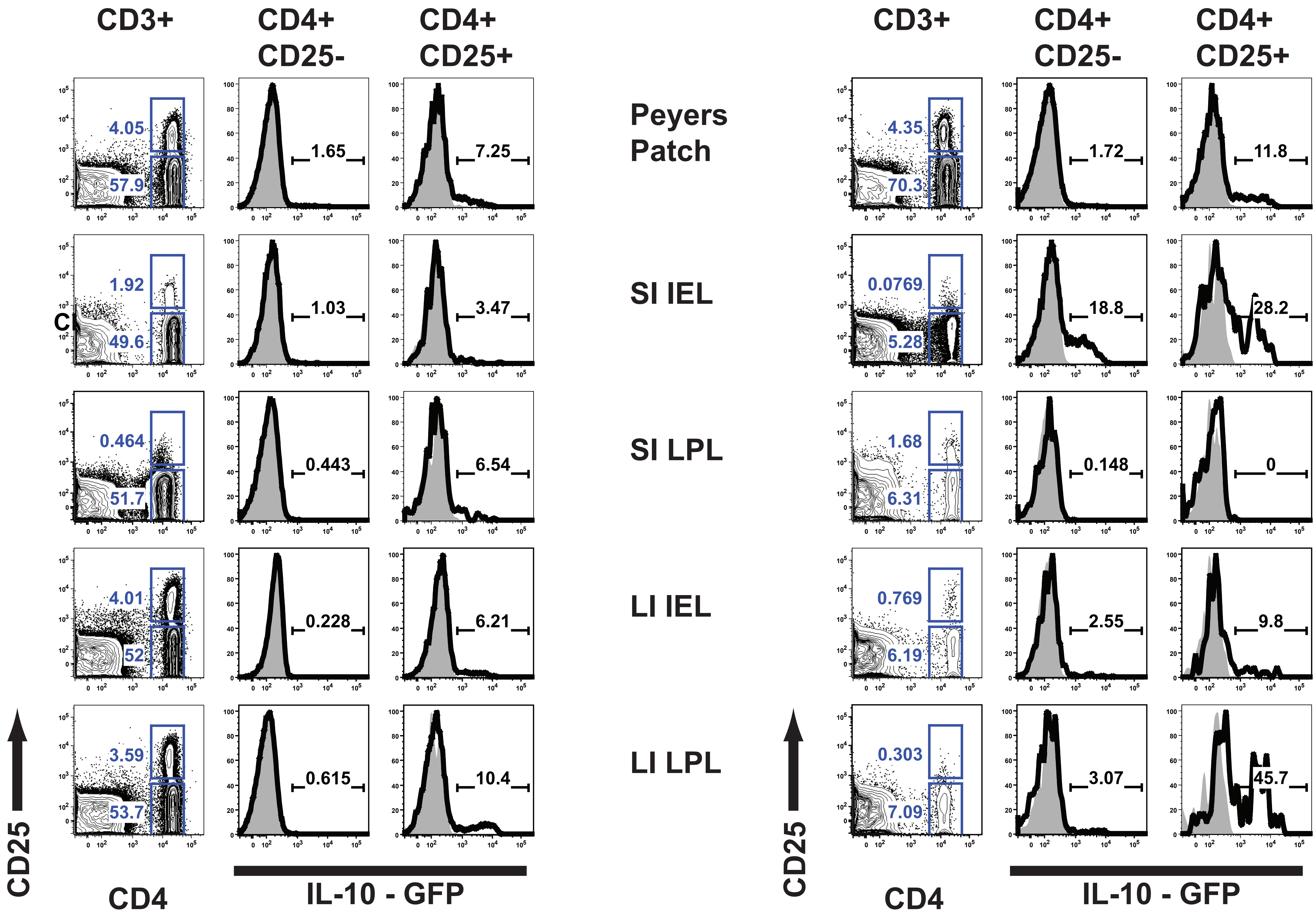

Supplemental Figure 2
Expression of *Il10* and *Il17* in B16-F10 melanoma

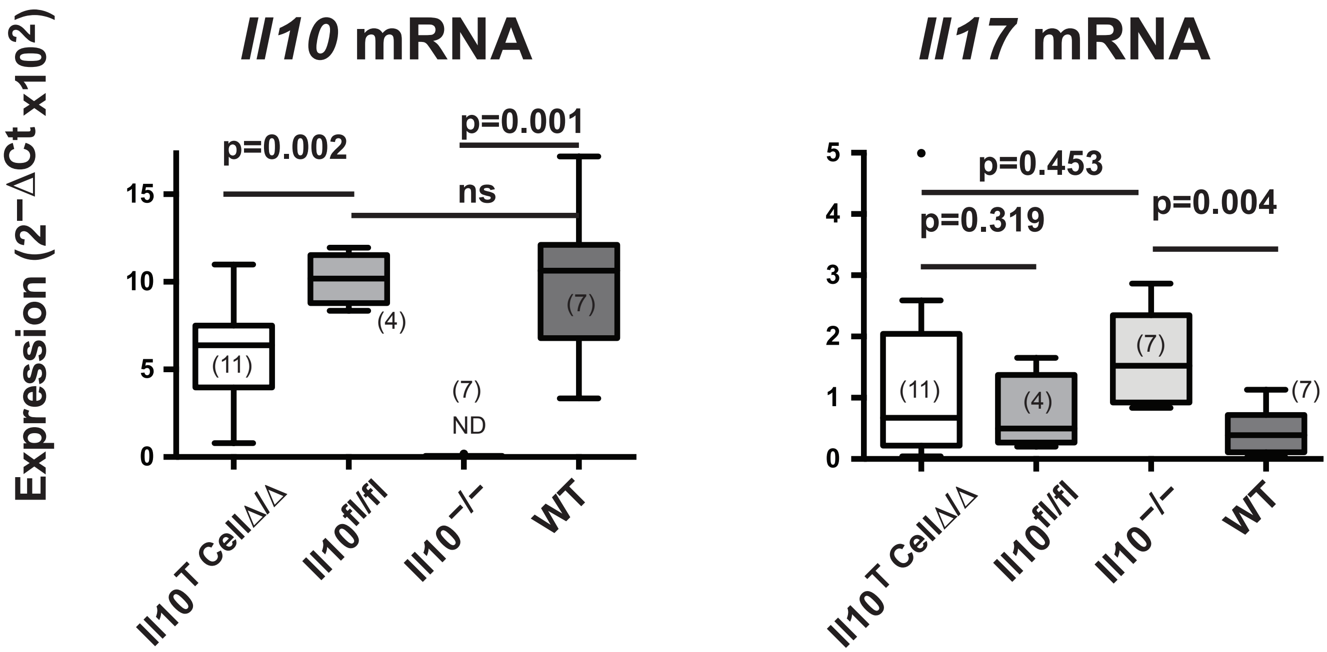

Supplemental Figure 3

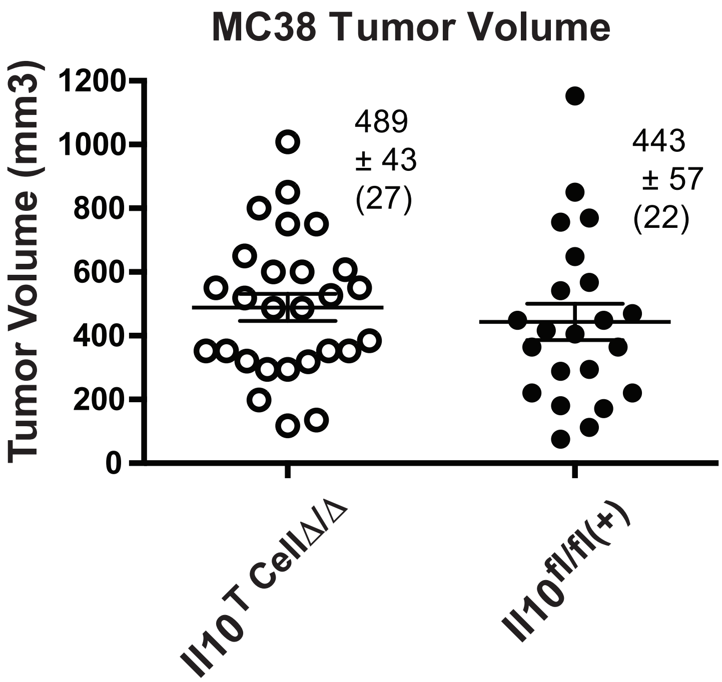

Supplemental Figure 4

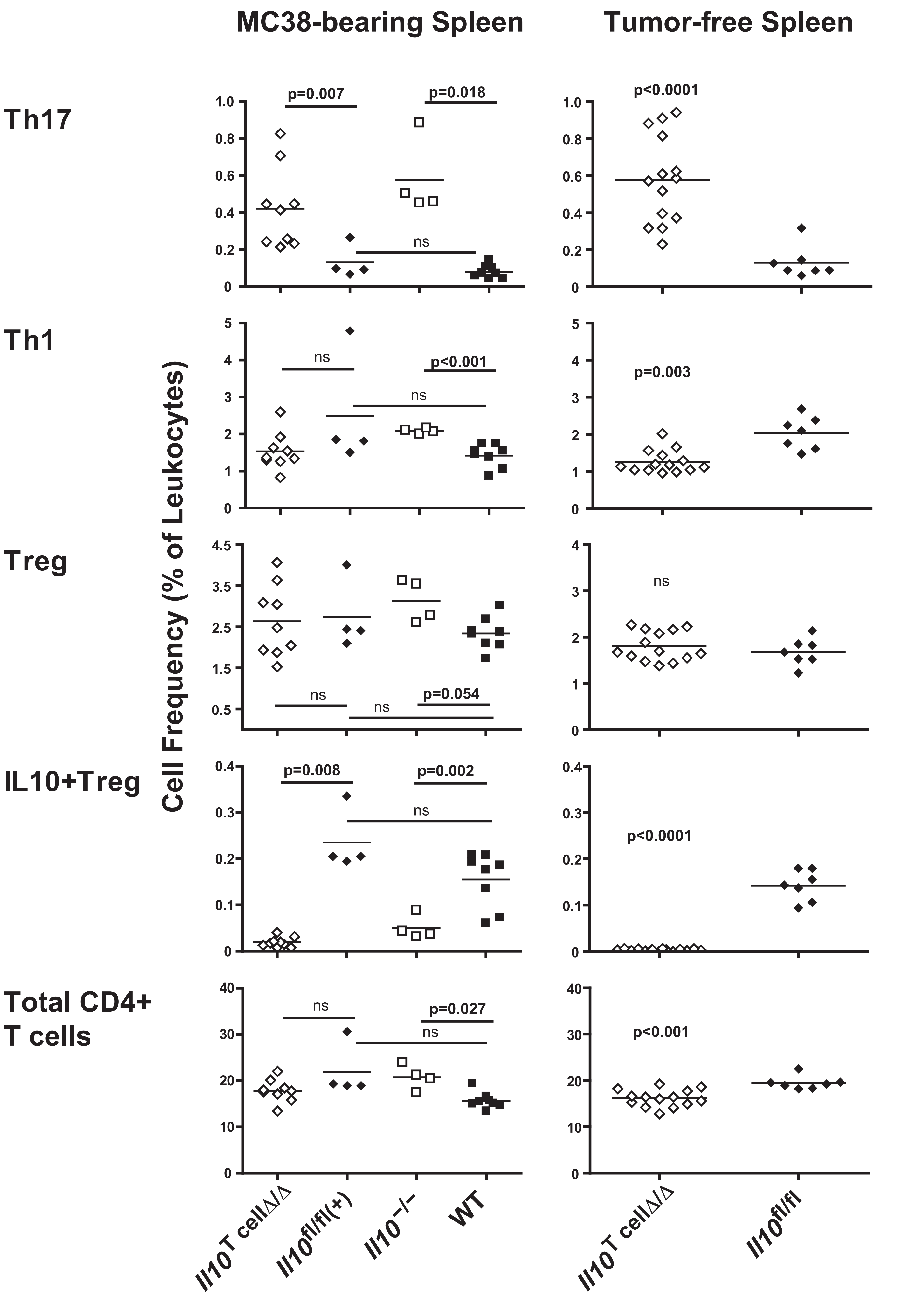

Supplemental Figure 5

Relationship between *Il10* and *Il17* expression in human HNSCC

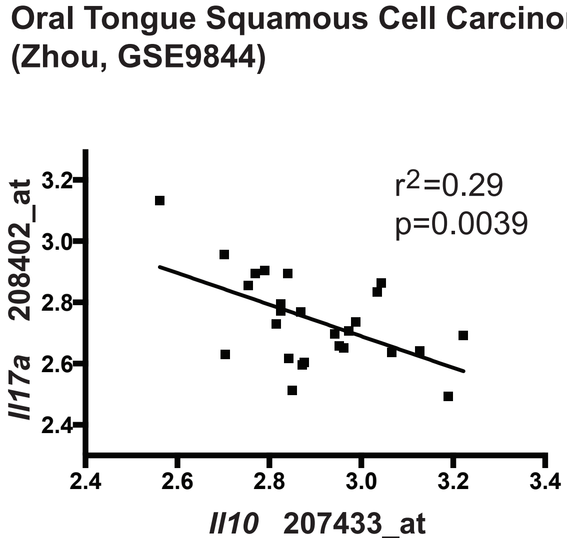

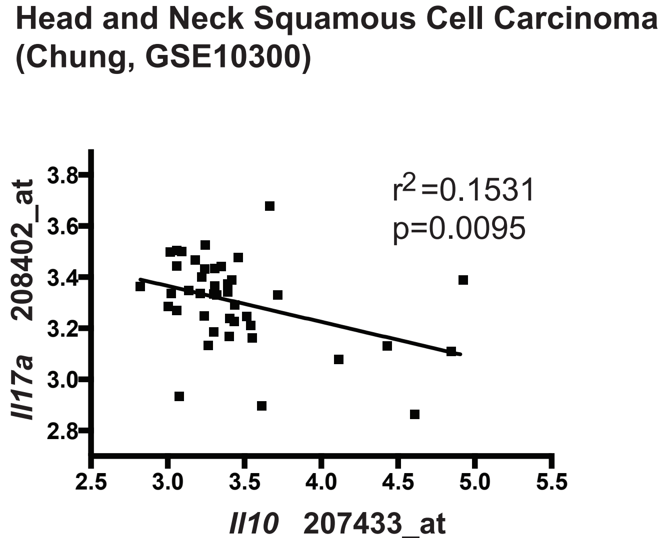

Supplemental Figure 6

A MC38 tumor Treg sort scheme

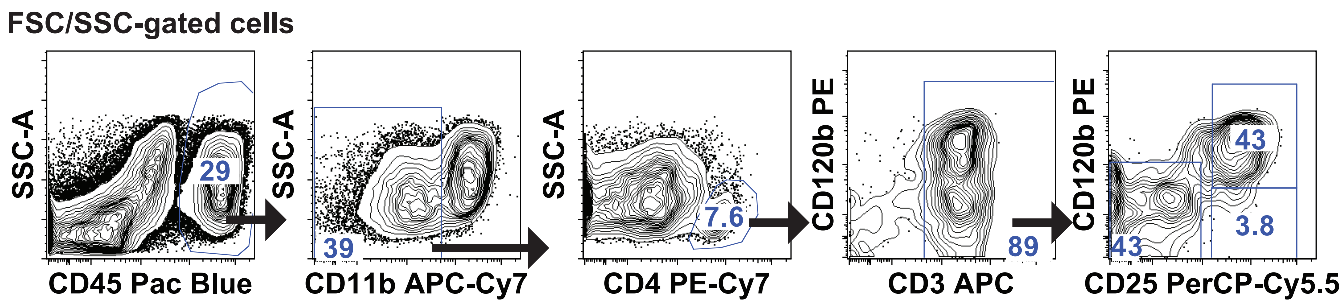

B FoxP3 expression by MC38 tumor CD4+ T cell populations

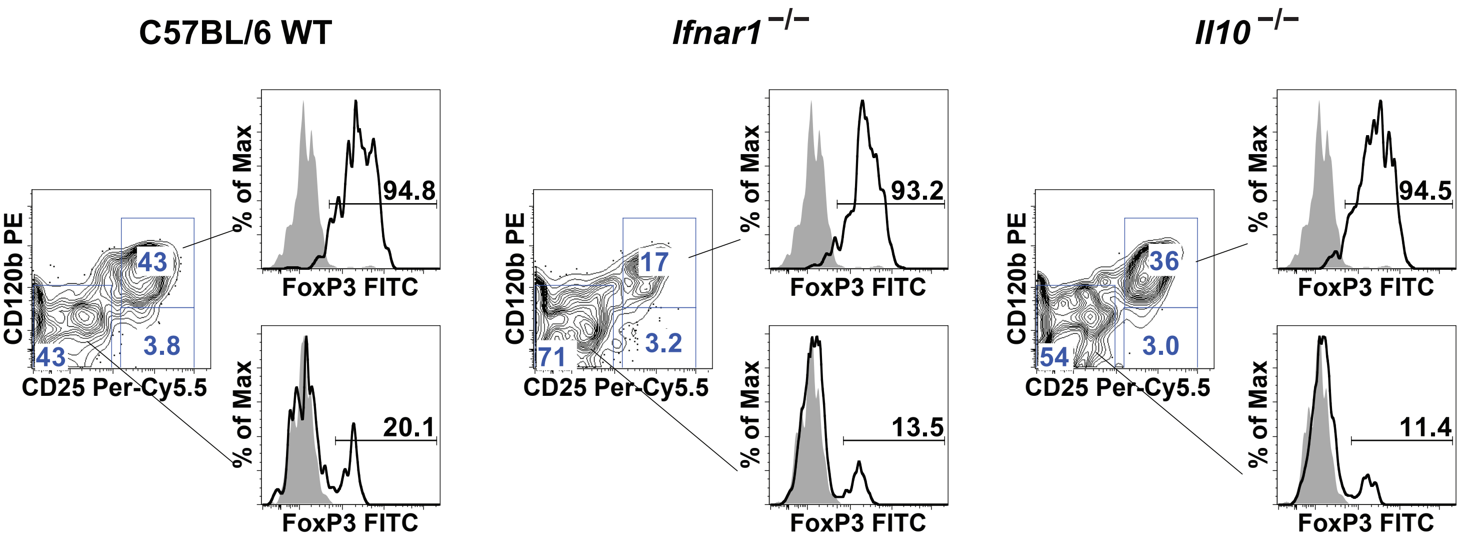

C Comparison of IL-10 mAb staining with IL-10GFP

VERT-X Mes LN CD4+ T cells

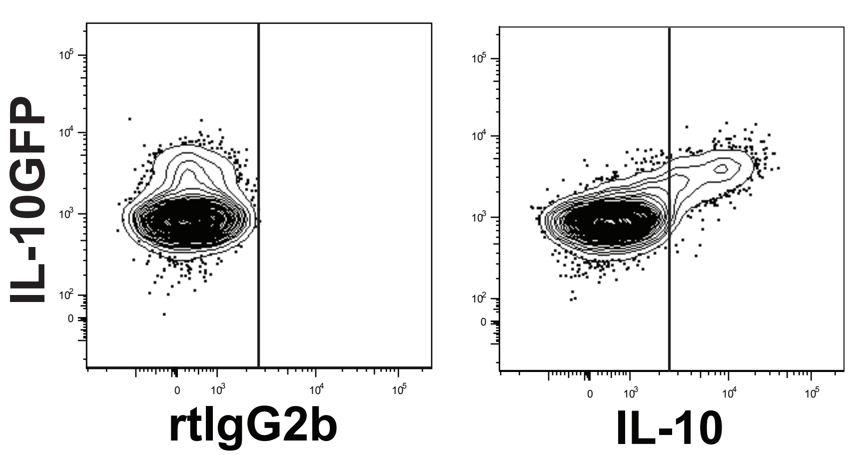

Supplemental Figure 7

Tumor Treg IL10GFP+ vs IL10GFP−

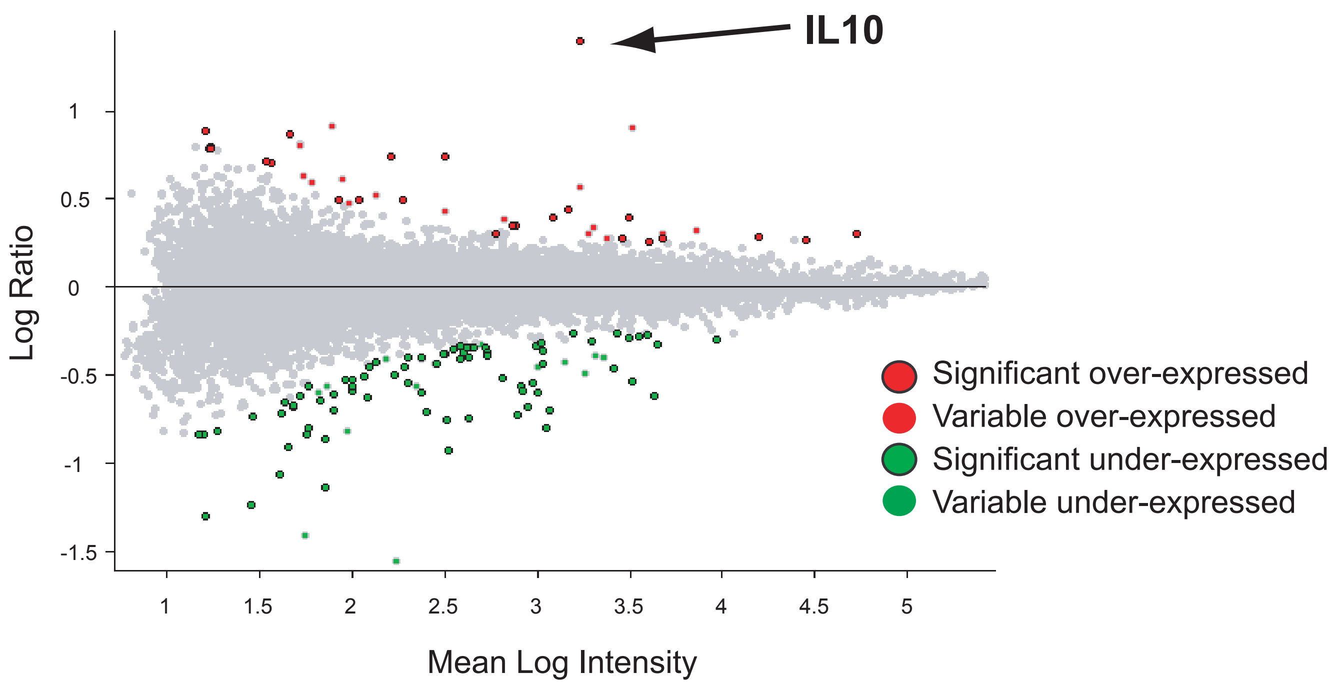

43 overexpressed, 93 underexpressed

FDR=0.5 and fold-change threshold=1

Supplemental Figure 8

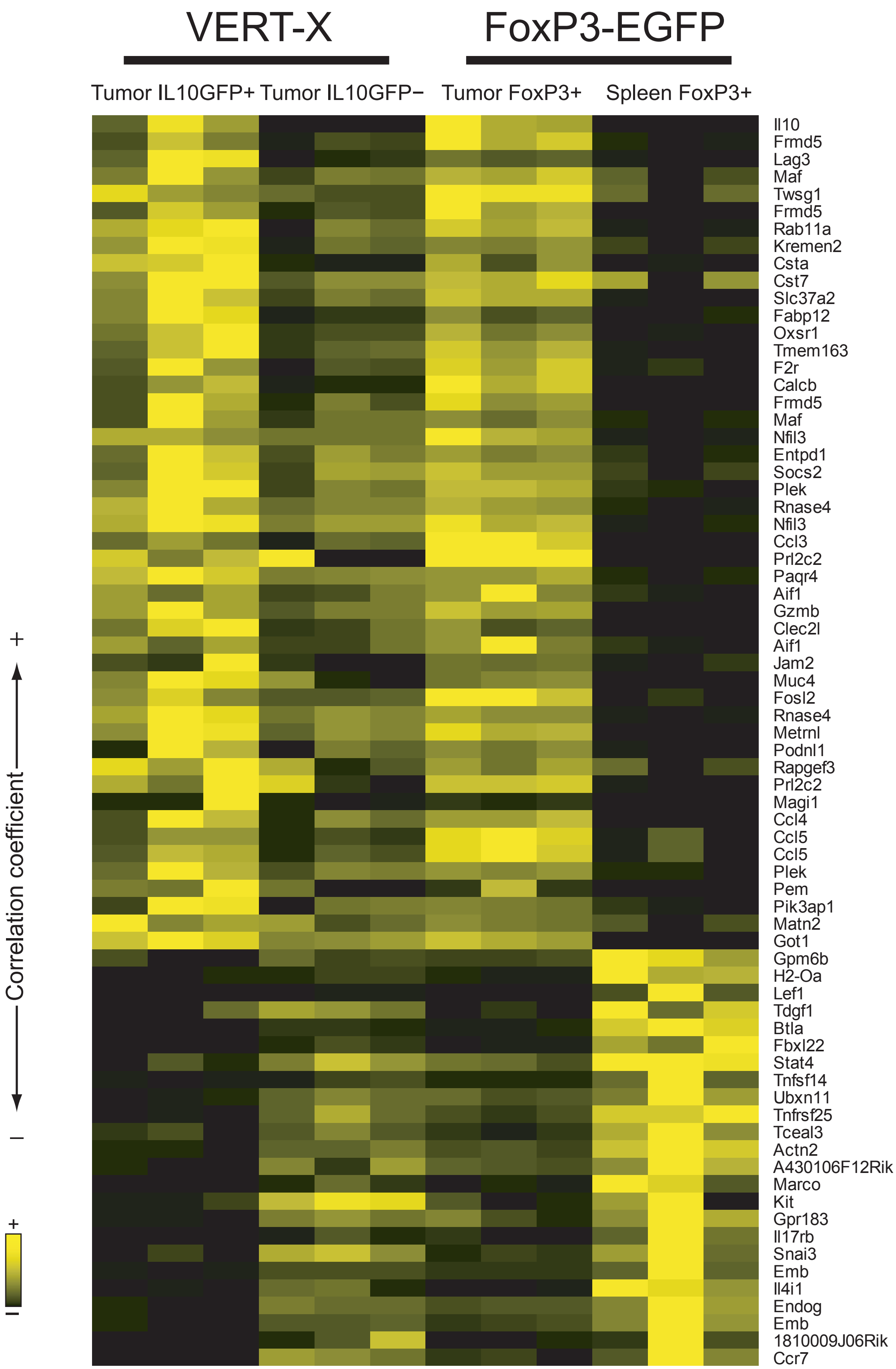

Supplemental Figure 9

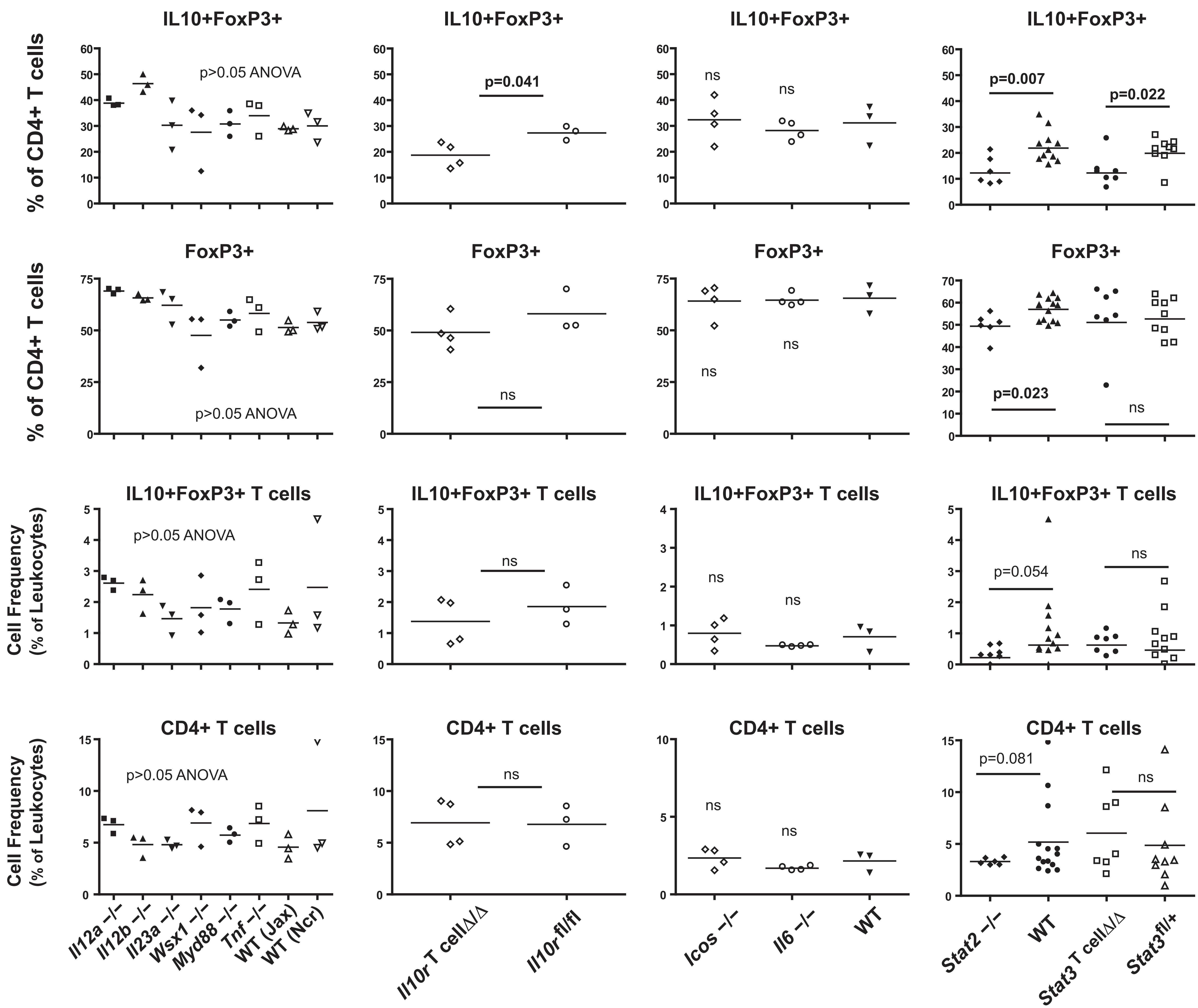

Supplemental Figure 10

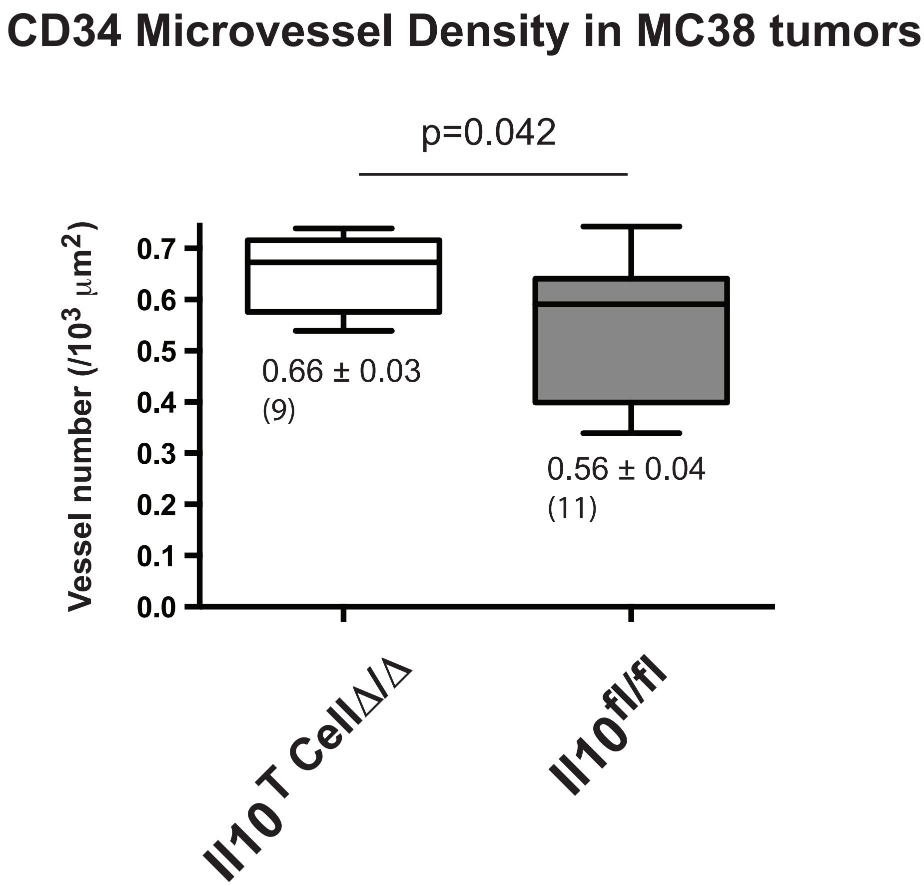

Supplemental Figure 11